0013-7227/07/$15.00/0
Printed in U.S.A.

Endocrinology 148(3):1050–1058

doi: 10.1210/en.2006-1600

Agonist-Induced Endocytosis of Rat Somatostatin Receptor 1

Dirk Roosterman, Oliver J. Kreuzer, Nicole Brune, Graeme S. Cottrell, Nigel W. Bunnett, Wolfgang Meyerhof,* and Martin Steinhoff*

Department of Dermatology (D.R., M.S.), Interdisziplinäres Zentrum für Klinische Forschung (IZKF) Münster, and Ludwig Boltzmann Institute for Cell and Immunobiology of the Skin, University of Münster, 48149 Münster, Germany; Department of Molecular Genetics (O.J.K., N.B., W.M.), German Institute of Human Nutrition Potsdam-Rehbruecke, 14558 Nuthetal, Germany; and Department of Surgery and Physiology (G.S.C., N.W.B.), University of California, San Francisco, San Francisco, California 94143-0660

Somatostatin-receptor 1 (sst1) is an autoreceptor in the central nervous system that regulates the release of somatostatin. Sst1 is present intracellularly and at the cell surface. To investigate sst1 trafficking, rat sst1 tagged with epitope was expressed in rat insulinoma cells 1046-38 (RIN-1046-38) and tracked by antibody labeling. Confocal microscopic analysis revealed colocalization of intracellularly localized rat sst1-human simplex virus (HSV) with Rab5a-green fluorescent protein and Rab11a-green fluorescent protein, indicating the distribution of the receptor in endocytotic and recycling organelles. Somatostatin-14 induced internalization of cell surface receptors and reduction of binding sites on the cell surface. It also stimulated recruitment of intracellular sst1-HSV to the plasma membrane. Confocal analysis of sst1-HSV revealed that the receptor was initially transported within superficial vesicles. Prolonged stimulation of the cells with the peptide agonist induced intracellular accumulation of somatostatin-14. Because the number of cell surface binding sites did not change during prolonged stimulation, somatostatin-14 was internalized through a dynamic process of continuous endocytosis, recycling, and recruitment of intracellularly present sst1-HSV. Accumulated somatostatin-14 bypassed degradation via the endosomal-lysosomal route and was instead rapidly released as intact and biologically active somatostatin-14. Our results show for the first time that sst1 mediates a dynamic process of endocytosis, recycling, and reendocytosis of its cognate ligand. (*Endocrinology* 148: 1050–1058, 2007)

THE TETRADECAPEPTIDE SOMATOSTATIN (SST)-14 and the N terminally extended form, sst-28, are major inhibitory peptides with broad endocrine, exocrine, and neuronal functions (1). The biological actions of somatostatin are mediated by five G protein-coupled receptors (GPCRs) (sst1, sst2, sst3, sst4, and sst5) (reviewed in Ref. 1). These receptor subtypes share common signaling pathways, which include inhibiting adenylyl-cyclase and modulating MAPK through G protein-dependent mechanisms (reviewed in Refs. 2 and 3). sst1 and sst2 also couple to voltage-dependent Ca^{2+} channels, tyrosine phosphatase SHP-1, and phospholipase A2 (4–8).

Several observations suggest that sst1 is an autoreceptor regulating the release of its own peptide agonist, somatostatin. The presence of sst1 mRNA in the periventricular nucleus of the hypothalamus, which is rich in somatostatin, suggests that both receptor and peptide colocalize, which may indicate an autoregulative function of the receptor (9, 10). Furthermore, the receptor and peptide colocalize in the somatostatinergic paraventricular neuronal system and in the retina of the rat (11, 12). Functional studies with receptor subtype-specific agonists or mice in which the sst1 gene is deleted underscore the autoregulative function of sst1 (13, 14).

We previously found that sst1 and sst2 are endogenously expressed in the rat insulinoma cell line 1046–38 (RIN 1046–38) (4). Displacement binding analysis and RT-PCR indicated that sst1 is the major somatostatin receptor subtype expressed in this cell line, in which it functionally couples to voltage-dependent Ca^{2+} channels (4, 15). Stimulation of epitope-labeled recombinant rat sst1-HSV with somatostatin induces loss of cell surface-binding sites in these cells, which is indicative of receptor endocytosis (15). sst1 has also been internalized in HEK293 cells (16), although some groups have shown that somatostatin either does not induce sst1 receptor endocytosis or causes very slow internalization [half-time ($T_{1/2}$) > 180 min] of this receptor (15–20). Thus, the possible mechanisms of endocytosis of sst1 are unknown.

Most studies of agonist-induced endocytosis of GPCRs have focused on clathrin-dependent mechanisms that involve dynamin and the clathrin adaptor molecule β-arrestin (reviewed in Ref. 21). Recently endocytosis of sst1 was shown not to be mediated by β-arrestin (22).

Here we report on the trafficking of sst1 and its cointernalized peptide agonist SST-14. Our findings indicate that peptide stimulation induces a fast dynamic process of endocytosis, recycling, and reendocytosis of the receptor and the ligand. SST-14 is not routed to lysosomal degradation; the ligand is continuously internalized and released as intact and

First Published Online December 14, 2006

* W.M. and M.S. contributed equally to this work.

Abbreviations: EGFP, Enhanced green fluorescent protein; FITC, fluorescein isothiocyanate; GPCR, G protein-coupled receptor; HSV, human simplex virus; sst, somatostatin-receptor; SST, somatostatin; $T_{1/2}$, half-time.

***Endocrinology* is published monthly by The Endocrine Society (http://www.endo-society.org), the foremost professional society serving the endocrine community.**

biological active SST-14 in the medium, in which it is cleaved by endopeptidases sensitive to phosphoramidon. Our findings also indicate that intracellular sst1 is involved in receptor-mediated uptake of SST-14.

Materials and Methods

Materials

SST-14 was obtained from Saxon Biochemicals (Bissendorf, Germany). ^{125}I-Tyr^{11}-SST-14 was from Amersham (Braunschweig, Germany) and FITC-labeled SST-14 was obtained from Advanced Bioconcept (Derry, Canada). Mouse antihuman simplex virus (HSV) glycoprotein D monoclonal antibodies were purchased from Novagen (Madison, WI). Media, sera, and plastics were from Life Technologies, Inc./BRL (Eggenstein, Germany). Lipofectamine 2000 was from Invitrogen (Karlsruhe, Germany). Unless otherwise specified, all other reagents were from Sigma (St. Louis, MO).

Generation of cDNA constructs and cell lines

All experiments used the rat insulinoma cell line 1046–38. This cell line endogenously expresses sst1$_{endo}$ with a maximal binding capacity of 31 (± 7) fmol per 2 × 10^4 cells. Sst1$_{endo}$ is functionally coupled to adenylyl-cyclase and voltage-dependent Ca^{2+} channels in these cells (4, 15). RIN-sst1-HSV cells were maintained in RPMI 1640 medium containing 400 μg/ml G418 and demonstrated a maximal binding capacity of 840 (± 90) fmol per 2 × 10^4 cells (15). Plasmids encoding sst1-HSV, and Rab5a-enhanced green fluorescent protein (EGFP), Rab11a-EGFP have been described (15, 23–25). RIN-sst1-HSV cells were transiently transfected with Lipofectamine 2000 and used 48 h after transfection.

Reduction of cell surface binding

Cells grown in 24-well dishes were stimulated with 1 μM SST-14 in RPMI 1640 medium (0.1% BSA) for 0–120 min at 37 C. Cells were placed on ice, washed three times with chilled acidic buffer, and incubated with 100,000 cpm per 0.3 ml ^{125}I-Tyr^{11}-SST-14, 0.01 nM SST-14, 0.1% BSA in RPMI 1640 medium, at 4 C for 90 min (15). Bound ^{125}I-Tyr^{11}-SST-14 was collected after lysing of the cells in 1 ml 1 M NaOH and determined in a γ-counter (Canberra Packard, Dreieich, Germany). Calculations and graphical presentation were carried out using Excel. Unspecific binding was determined in the presence of 0.1 mM SST-14.

Receptor-mediated uptake of ^{125}I-Tyr^{11}-SST-14

RIN-sst1-HSV cells grown in 24-well microtiter dishes were incubated with 100,000 cpm per 0.3 ml ^{125}I-Tyr^{11}-SST-14 mixed with 0.01 nM SST-14 in RPMI 1640 medium (0.1% BSA) at 37 C in the presence or absence of 40 mM ammonium chloride (pH 7.4), monensin (50 μM), or sucrose (0.45 M) (26). After 0–120 min, the cells were placed on ice and washed with chilled acidic buffer [Hank's salt solution, 20 mM acetic acid (pH 4.75)] (15). Cells were lysed in 1 M NaOH and radioactivity was measured in a γ-counter.

Displacement binding assay

Cells, seeded in 24-well microtiter plates, were incubated on ice with 100,000 cpm per 0.3 ml ^{125}I-Tyr^{11}-SST-14 containing indicated concentrations of unlabeled SST-14 in RPMI 1640 medium and 0.1% BSA at 4 C for 90 min. Cells were washed with chilled RPMI 1640 and 0.1% BSA, lysed in 1 ml 1 M NaOH, and surface-bound ^{125}I-Tyr^{11}-SST-14 was determined in a γ-counter.

Displacement uptake assay

Cells, seeded in 24-well microtiter plates, were stimulated with 100,000 cpm per 0.3 ml ^{125}I-Tyr^{11}-SST-14 containing 0.01–1000 nM SST-14 in RPMI 1640 medium and 0.1% BSA at 37 C for 75 min. Cells were washed with chilled acidic buffer (pH 5.0), lysed in 1 M NaOH, and cell-associated radioactivity determined in a γ-counter.

HPLC analysis of ^{125}I-Tyr^{11}-SST-14

Cells were incubated with 100,000 cpm/ml ^{125}I-Tyr^{11}-SST-14 in RPMI 1640 and 0.1% BSA in the presence or absence of 10 μM phosphoramidon at 37 C. After 10 min of stimulation, cells were placed on ice and washed twice with chilled acidic buffer (pH 5.0) (15). Cells were washed once with chilled RPMI 1640 and 0.1% BSA, incubated for the indicated times at 37 C in 1 ml RPMI 1640 and 0.1% BSA, and placed on ice. The supernatants were collected and acidified by adding 10 μl trifluoroacetic acid. The supernatants were centrifuged (5 min, 13,000 × *g*) and subjected to HPLC separation. Cell-associated radioactivity was determined by adding 1 ml HPLC buffer A. Lysed cells were centrifuged (5 min, 13,000 × *g*) and subjected to HPLC separation.

HPLC was done on a reverse-phase C-18 column (2 × 25 mm). A separating gradient of 0–40% acetonitrile, 0.08% trifluoroacetic acid, 25 min, 1 ml/min was performed with a HPLC-Model Gold (Beckman, Krefeld, Germany). The HPLC gradient was fractionated every minute, and the eluted radioactivity was determined in a γ-counter (27, 28). The radioactivity of each fraction was divided by the initial amount of cell-associated radioactivity determined after 10 min of incubation with 100,000 cpm/ml ^{125}I-Tyr^{11}-SST-14.

Recycling of ^{125}I-Tyr^{11}-SST-14

Cells were stimulated with 100,000 cpm/ml ^{125}I-Tyr^{11}-SST-14 mixed with 0.01 nM unlabeled SST-14 in RPMI1640 and 0.1% BSA at 37 C. After 10 min, dishes were placed on ice and cells were washed three times with chilled acidic buffer. Cells were then washed once with chilled RPMI 1640 and 0.1% BSA and incubated at 37 C. Medium was exchanged with 1 ml fresh temperate medium after 1, 5, 10, 15, and 30 min of incubation and the amount of recycled radioactivity was quantified in a γ-counter.

Determination of SST-14-mediated inhibition of adenylyl cyclase activity

RIN-sst1-HSV cells were stimulated for 15 min with 1 μM SST-14, placed on ice and washed twice with chilled acidic buffer and once with chilled RPMI 1640 and 0.1% BSA. Thereafter cells were incubated at 37 C. After 10 min, supernatant was collected. The method for determining inhibition of forskolin-stimulated adenylyl-cyclase of the supernatant has been described elsewhere (15).

Surface biotinylation of RIN-sst1 cells

Proteins located on the cell surface were biotinylated according to manufacturer's instructions (Pierce, Bonn, Germany). Briefly, cells grown on glass coverslips were placed on ice, washed with chilled PBS adjusted to pH 8.0, and incubated for 30 min with 5 mM sulfo-NHS-LC-biotin (Pierce) in PBS (pH 8.0) at 4 C. Thereafter the cells were washed once with PBS (pH 8.0) and 50 mM glycine and then with chilled RPMI 1640 and 0.1% BSA. They were then stimulated with SST-14 (10 nM). The localization of sst1-HSV was analyzed by confocal microscopy.

Microscopy and immunofluorescence

Cells were stimulated with 10 nM SST-14 or fluorescein isothiocyanate (FITC)-SST14 in RPMI 1640 medium and 0.1% BSA for the indicated times at 37 C, washed with Hank's-buffered saline/acetic acid (pH 4.75) at 4 C, fixed, and permeabilized for 30 min in Hank's-buffered saline, 5% normal goat serum, and 0.05% saponin. sst1-HSV was detected by using mouse anti-glycoprotein D antibody (1:10,000, overnight at 4 C). Biotinylated proteins were detected by using Texas Red-conjugated streptavidin (1:2000, 1 h, room temperature), Rab-proteins by using green fluorescent protein fluorescence, and SST-14 by FITC-SST-14. FITC-conjugated or Texas Red-conjugated goat antimouse IgG was used as secondary antibodies (1:200, 1 h, room temperature). Cells were embedded in Vectashield mounting medium (Vector, Burlingame, CA) and observed with confocal microscopy (15).

Results

Acidic washes remove surface-bound ligand

To differentiate between cell surface-bound and cell-associated ^{125}I-Tyr^{11}-SST-14, cells were washed with chilled

acidic buffer. The effect of acid treatment on RIN-sst1-HSV cells stimulated at 37 C or incubated at 4 C with 100,000 cpm ^{125}I-Tyr^{11}-SST-14 is shown in Table 1. Cell surface-bound ^{125}I-Tyr^{11}-SST-14 was nearly completely removed after three washes, whereas cell-associated ^{125}I-Tyr^{11}-SST-14 was located in acidic wash-resistant compartments (Table 1).

Stimulation with SST-14 induced loss of cell surface binding sites

We determined the specificity of sst1 internalization by quantification of the agonist-induced loss of cell surface binding sites in untransfected RIN-1046–38 cells (Fig. 1A) and RIN-1046–38 stable expressing sst1-HSV (Fig. 1B). At 4 C, unstimulated RIN-1046–38 cells bound approximately 800 ($\pm$ 250) cpm per 2×10^4 cells, whereas unstimulated RIN-sst1-HSV cells bound more than 10 times as much ligand [approximately 8500 ($\pm$ 250) cpm per 2×10^4]. After exposure to SST-14, cell surface binding sites rapidly decreased in both cell lines. During the first 2–5 min of stimulation, binding sites dropped to 50% of the original value and remained at this level throughout the experiment.

sst1 mediates uptake of ^{125}I-Tyr^{11}-SST-14

Receptor-mediated uptake of ^{125}I-Tyr^{11}-SST-14 was characterized by chronic stimulation of the cells with the agonist. During the first 2–3 min of stimulation, RIN-1046–38 cells accumulated approximately 400 cpm per 2×10^4 cells, whereas RIN-sst1-HSV cells accumulated more than 10 times that much (5000 cpm per 2×10^4; Fig. 1, C and D). After 2–3 min of stimulation, the amount of accumulated radioactivity was equivalent to 50% of surface-bound ^{125}I-Tyr^{11}-SST-14 at 4 C (compare Fig. 1, A and B, with Fig. 1, C and D). After 75 min of stimulation, cell-associated radioactivity reached the maximal level of 220% of the cell surface binding sites (Fig. 1, C and D). These results show that recombinant sst1-HSV and endogenously expressed sst1 demonstrate identical kinetics concerning loss of cell surface binding sites and receptor-mediated uptake of the ligand. They also indicate that epitope-labeled sst1-HSV and endogenously expressed sst1 behave identically.

To further characterize the sst1-specific uptake of SST-14 we stimulated the cells in the presence of 0.45 M sucrose, which inhibits the clathrin-mediated and the caveolin-mediated receptor endocytosis (29, 30). We found that sucrose nearly completely inhibited sst1-mediated uptake of SST-14 (Fig. 1E). Receptor trafficking was further characterized by neutralizing acidic cell compartments with ammonium chloride (26). We found that sst1-mediated accumulation of SST-14 was not affected, suggesting that vesicular acidification is not important for the accumulation of SST-14 (26). Control experiments simultaneously performed in RIN-sst3-HSV cells demonstrated that preincubation with ammonium chloride efficiently blocked receptor trafficking and lysosomal degradation of SST-14 and thereby changed the kinetics of sst3-mediated uptake of SST-14 (data not shown). To inhibit trafficking of sst1 from perinuclear membrane structures, the Golgi apparatus and post-Golgi endosomes were disrupted by the cationophor monensin (31). Monensin (50 μM) markedly inhibited sst1-mediated accumulation of SST-14, even at early time points of stimulation (Fig. 1E), suggesting that recruitment of intracellular sst1-HSV is needed for continuous accumulation of the ligand. To investigate whether monensin or sucrose influenced receptor surface binding, RIN-sst1-HSV cells were incubated with monensin or sucrose (Fig. 1F) and surface binding sites were determined by incubating the cells with 100,000 cpm ^{125}I-Tyr^{11}-SST-14 for 90 min at 4 C. Treatment with monensin and sucrose did not change surface binding sites of RIN-sst1-HSV (Fig. 1F), which suggests that the induced recruitment of intracellular sst1 is essential for the continuous accumulation of the ligand.

TABLE 1. Removal of surface-bound peptide by acidic washes.

Temperature (C)	Bound (cpm)	Acidic extractable (%)
37	22.400 $\pm$ 400	21 $\pm$ 1
4	8.500 $\pm$ 250	96 $\pm$ 3

RIN-sst1-HSV cells were incubated with ^{125}I-Tyr^{11}-SST-14 (100,000 cpm) for 90 min at the indicated temperature. The amount of bound ^{125}I-Tyr^{11}-SST-14 was then determined before and after treatment of the cells with three acidic washes [Hank's salt solution, 20 mM acetic acid (pH 4.75)], as described in *Materials and Methods*.

Displacement binding assays

To further clarify the process of sst1-mediated uptake of SST-14, we performed displacement binding assays at 4 C and displacement uptake assays at 37 C (Fig. 1G). At all concentrations of SST-14, the amount of cell-associated ^{125}I-Tyr^{11}-SST-14 was approximately 2.2 times the amount of cell surface-bound ligand. The Scatchard plot (not shown) demonstrated a dissociation constant$_{(4\ C)}$ of 2.5 $\pm$ 1.0 nM and dissociation constant$_{(37\ C)}$ of 2.5 $\pm$ 1.0 nM. The cell surface-binding sites for RIN-sst1 cells were determined to be 840 $\pm$ 90 fmol per 2×10^4 cells, whereas the maximal amount of accumulated SST-14 was determined to be 1750 $\pm$ 110 fmol per 2×10^4 cells.

Comparison of the kinetics of the agonist-induced loss of cell surface binding sites and the sst1-mediated uptake of SST-14

Both methods are used to determine agonist-induced internalization of sst1 (15, 17, 20). Therefore, we merged the curves obtained from agonist-induced loss of cell surface binding sites (Fig. 1B) and the curve from sst1-mediated uptake of SST-14 (Fig. 1D). After 2–3 min of stimulation, both curves crossed at approximately 4700 cpm (Fig. 1H, *arrow*); 4700 cpm is equal to 50% of cell surface bound ligand of unstimulated cells. Therefore, after approximately 3 min of incubation 50% of ligand occupied sst1 are internalized when stimulated with 1 μM SST-14 (Fig. 1B). Moreover, 50% of ligand occupied sst1 are internalized when stimulated with 0.01 nM SST-14 (Fig. 1D). Therefore, the process of agonist-induced internalization of sst1 is independent from the concentration of the ligand. To determine $t_{1/2}$ for the receptor mediated uptake of SST-14, the initial speed of this process was linearized by setting a tangent (Fig. 1D, *dotted line*). We calculated $t_{1/2}$ = 2.0 min for this process. Interestingly, after 3 min of stimulation, the amount of cell-associated ^{125}I-Tyr^{11}-SST-14 exceeded 4700 cpm. This observation indicates a dy-

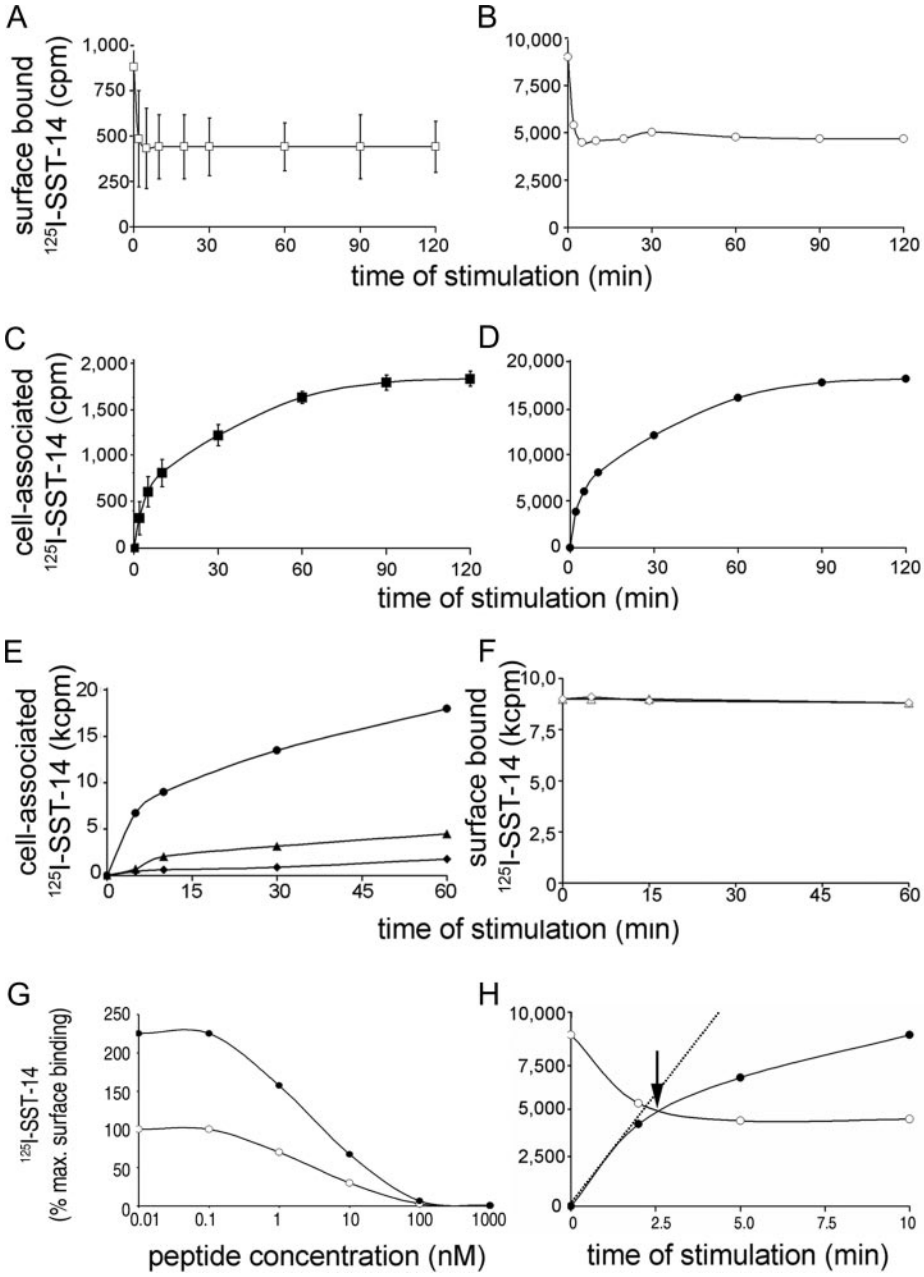

FIG. 1. SST-14-induced endocytosis of sst1. SST-14-mediated reduction of cell surface binding sites (A and B). RIN-1046–38 cells (A) and RIN-sst1-HSV cells (B) were stimulated with SST-14 (1 μM) at 37 C for the indicated times. After three acidic washes, cell surface binding sites were determined by incubating the cells with 100,000 cpm radioactive SST-14 at 4 C. During the first 2–3 min after stimulation, SST-14 induced a 50% loss of cell surface binding sites. sst1 mediated accumulation of SST-14 (C and D). RIN-1046–38 cells (C) and RIN-sst1-HSV cells (D) were incubated at 37 C with ^{125}I-Tyr^{11}-SST-14 for the indicated time points. Surface-located ^{125}I-Tyr^{11}-SST-14 was washed off with three acidic washes, and the amount of cell-associated radioactivity was determined in a γ-counter. sst1-HSV-specific uptake of ^{125}I-Tyr^{11}-SST-14 in the presence of ammonium chloride (*circles*), monensin (*triangles*), and sucrose (*diamonds)* (E). Cells were stimulated at 37 C with 100,000 cpm ^{125}I-Tyr^{11}-SST-14 in the presence of ammonium chloride (40 mM), monensin (50 μM), or sucrose (0.45 M) for the indicated time points. After three acidic washes, cell-associated radioactivity was determined. sst1-specific uptake of ^{125}I-Tyr^{11}-SST-14 was not influenced through neutralization of acidic vesicles by ammonium chloride. Treatment of cells with monensin inhibited accumulation of ^{125}I-Tyr^{11}-SST-14. Stimulation of cells in the presence of sucrose almost completely blocked uptake of ^{125}I-Tyr^{11}-SST-14. F, Influence of monensin (*circles*) and sucrose (*triangles*) on cell surface binding sites. Cells were stimulated with monensin (50 μM) or sucrose (0.45 M) at 37 C for the indicated times. Cells were washed and cell surface binding sites were determined by incubation with ^{125}I-Tyr^{11}-SST-14 at 4 C. Cell surface binding sites did not change during incubation with monensin or sucrose. G, Displacement of ^{125}I-Tyr^{11}-SST-14 cell surface binding and uptake by unlabeled somatostatin in RIN-sst1-HSV cells. Radioactive labeled SST-14 was mixed with the indicated concentration of unlabeled SST-14. *Open circles* show cell surface binding of ^{125}I-Tyr^{11}-SST-14 (90 min, 4 C). *Closed circles* show the specific amount of cell-associated radioactivity after stimulation (75 min, 37 C). The amount of cell-associated radioactivity was 2.2 times the amount of specifically surface-bound ^{125}I-Tyr^{11}-SST-14. Comparison of sst1-mediated uptake of ^{125}I-Tyr^{11}-SST-14 and SST-14 induced loss of cell surface binding sites (H). Data from B and D were merged. After 2–3 min, both graphs crossed at approximately 4700 cpm (*arrow*), which is equal to 50% of surface binding sites of unstimulated cells (*arrow*). *Dotted line* demonstrate the tangent of the initial uptake process. Errors are smaller than the symbols.

namic process. The data led us to conclude either that agonist stimulation induced rapid mobilization of intracellular sst1 or that one cycle of sst1 endocytosis and recycling takes place within this period of time.

SST-14 accumulates as intact peptide

The internalized radioactive peptides were characterized by HPLC. Figure 2A displays the time-dependent distribution of radioactive products that were found in the supernatant of RIN-sst1-HSV cells or were extracted from them. At all time points investigated, only ^{125}I-Tyr^{11}-SST-14 was detected cell-associated (Fig. 2, *closed circles*). Cell-associated ^{125}I-Tyr^{11}-SST-14 and reference ^{125}I-Tyr^{11}-SST-14 eluted at 20–21 min (data not shown). The amount of accumulated ^{125}I-Tyr^{11}-SST-14 rapidly dropped after replacement of the medium and then moderately declined during prolonged incubation times. This decrease in the quantity of intracellular peptide paralleled the increasing concentrations of intact peptide in the extracellular medium. During the first 5 min of incubation, cells released 35% of the internalized ^{125}I-Tyr^{11}-SST-14 into the supernatant (Fig. 2A). The ^{125}I-Tyr^{11}-SST-14 detected in the supernatant rapidly dissociated from the cells at pH 7.4. The amount of extracellular ^{125}I-Tyr^{11}-SST-14 slowly decreased during further incubation. Concomitant with this decrease, a radioactive-labeled degradation product of ^{125}I-Tyr^{11}-SST-14 was detected in the supernatant from 5 min after the incubation period onward (Fig. 2A). The amount of degraded peptide increased to 44% at 60 min of incubation. The degraded radioactive-labeled peptide (elution time 10–11 min) was likely obtained through hydrolysis of ^{125}I-Tyr^{11}-SST-14 by a neutral endopeptidase-like activity (27, 28). During chronic stimulation, SST-14 accumulated as intact SST-14 in the cells and was released as intact peptide into the extracellular medium. The released peptide was extracellularly degraded by endopeptidase-like activity. No radioactive degradation products could be detected cell-associated indicating that SST-14 did not lead to lysosomal degradation. These results suggested that during stimulation, SST-14 is dynamically endocytosed, recycled and reendocytosed as intact peptide. To explore this further, the incubation medium was repeatedly exchanged to suppress reendocytosis of the ligand under conditions in which SST-14 degradation was blocked by pretreatment of the cells with phosphoramidon to inhibit neutral endopeptidase-like activity. No radioactive degradation products were detected in the supernatant (Fig. 2B).

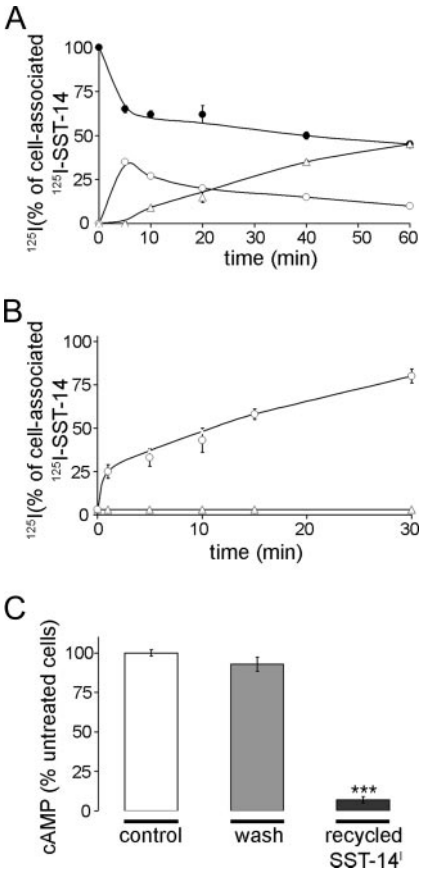

FIG. 2. Characterization of the cell-associated radioactivity. Distribution of ^{125}I-Tyr^{11}-SST-14 between RIN-sst1-HSV cells and the extracellular medium (A). Cells were stimulated with ^{125}I-Tyr^{11}-SST-14 (10 min, 37 C), washed with acidic buffer, and incubated for the indicated time points at 37 C. *Closed circles*, ^{125}I-Tyr^{11}-SST-14 in the cellular lysate; *open circles*, ^{125}I-Tyr^{11}-SST-14 in the extracellular medium; *triangles*, ^{125}I-Tyr^{11}-SST-14 degradation product in the extracellular medium. Cell-associated ^{125}I-Tyr^{11}-SST-14 was rapidly released as intact SST-14 and was slowly degraded in the medium. Distribution of ^{125}I-Tyr^{11}-SST-14 between RIN-sst1-HSV cells and the extracellular medium after repeated refreshing of medium (B). Cells were stimulated with ^{125}I-Tyr^{11}-SST-14 (10 min, 37 C) and washed with acidic buffer. To demonstrate that released ^{125}I-Tyr^{11}-SST-14 was reendocytosed by sst1, extracellular medium was refreshed at the indicated time points. Significantly more ^{125}I-Tyr^{11}-SST-14 was found extracellularly after the medium was repeatedly refreshed. Determination of the biological activity of recycled SST-14 (C). RIN-sst1-HSV cells stimulated with SST-14 (1 μM, 15 min, 37 C), were washed three times with acidic buffer and incubated for 10 min. The biological activity of recycled SST-14 was determined by inhibition of forskolin-stimulated adenylyl-cyclase in RIN-sst3 cells. The washing medium did not inhibit adenylyl-cyclase (*gray bar*). Recycled SST-14 was biologically active (*black bar*).

During repeated exchange of the medium, 22% (±3%) of cell-associated SST-14 was detected after 1 min, and 77 (±4%) after 30 min of incubation. Thus, these conditions allowed significantly more SST-14 to recycle into the medium. Taken together, these results indicate that recycled SST-14 was reendocytosed. In addition, the release of intact SST-14 underscores the observation that SST-14 does not lead to lysosomal degradation. The ligand is degraded by an endopeptidase sensitive to phosphoramidon.

Recycled SST-14 is biologically active

The HPLC results indicated that recycled SST-14 elutes at the same time as intact SST-14. To verify that recycled SST-14 is biologically active, the supernatant was tested to inhibit forskolin-stimulated adenylyl-cyclase activity. We compared the biological activity of the final washing buffer after stimulating RIN-sst1-HSV cells with SST-14 (1 μM, 10 min, 37 C) and the medium after 10 min of recycling (Fig. 2C). Only the culture medium from RIN-sst1-HSV cells inhibited cAMP formation by 92.9% (±4.5%); the washing medium was ineffective and reduced cAMP formation by only 7% (±2%). This finding supports the results we obtained by HPLC. Both sets of results indicate that intact and biologically active

SST-14 accumulates during chronic stimulation and is specifically released from RIN-sst1-HSV cells.

Agonist-induced trafficking of sst1-HSV

sst1-mediated uptake of FITC-SST-14. Our results did not allow us to clearly differentiate whether the dynamic process of sst1-mediated uptake of SST-14 was performed by rapid recycling of sst1 or by mobilization of intracellular sst1. Therefore, we analyzed sst1 trafficking by localizing FITC-SST-14 with confocal microscopy (Fig. 3A). Incubation at 37 C induced a significant uptake of FITC-SST-14. At all time points, FITC-SST-14 was observed in compartments located directly beneath the plasma membrane, suggesting that SST-14 accumulated in superficial vesicles. These findings are in line with uptake assays of FITC-SST-14 mediated by the human sst1 obtained in COS-7 cells (18).

SST-14 induced endocytosis of sst1-HSV. In untreated cells, sst1 demonstrated an intense intracellular distribution, which prevented microscopic discrimination of endocytosed sst1-HSV from intracellular sst1-HSV (15, 19, 22). To circumvent this problem, the plasma membrane proteins were biotinylated *in vivo* before we stimulated endocytosis of sst1. Thus, endocytosed proteins were detected by Texas Red coupled to streptavidin and sst1-HSV was detected by the FITC fluorescence of the sst1-HSV immunostaining (Fig. 3B). In untreated cells (30 min, 37 C, without SST-14), sst1-HSV was localized at the cell surface and in intracellular organelles, whereas biotinylated surface proteins were exclusively located at the cell surface (Fig. 3B, *top panels*). Localization of sst1-HSV in nonstimulated cells is in line with previous studies (15, 19, 22). Biotinylated proteins and sst1-HSV were observed colocalized in superficial vesicular compartments 15 min after stimulation with SST-14 (Fig. 3B, *middle panels*). Biotinylated proteins and sst1-HSV remained colocalized in superficial vesicular compartments at the cell surface 30 min after stimulation and were also found colocalized in vesicles scattered throughout the cell (Fig. 3B, *bottom panels*). Biotinylated proteins and sst1-HSV were located in superficial vesicles in a similar way as internalized FITC-SST-14 (Fig. 3A). In marked contrast to endocytosed FITC-SST-14, internalized proteins were detected scattered throughout the cell. These findings suggest that the internalized proteins separate from SST-14 in superficial vesicles or that FITC-SST-14 is not transported in the same way as the unlabeled ligand. Biotinylated proteins and sst1-HSV were transported into a superficial cell compartment (Fig. 3, C and D).

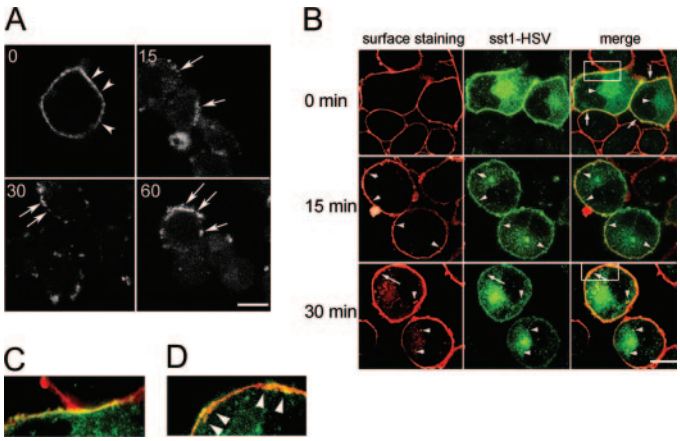

FIG. 3. FITC-SST-14 and sst1-HSV internalized into a superficial compartment. Uptake of FITC-SST-14 into a superficial cell compartment (A). RIN-sst1-HSV cells were stimulated for 90 min on ice with FITC-SST-14 (10 nM) and incubated for the indicated time points at 37 C. FITC-SST-14 accumulated within compartments localized directly beneath the plasma membrane (*arrows*). SST-14 induced internalization of cell surface-biotinylated proteins (B). Cells were stimulated with SST-14 (10 nM) for the indicated time points. *Red*, Surface proteins; *green*, sst1-HSV. The *right panels* demonstrate the overlay of both images. In untreated cells, sst1 was localized in intracellular vesicular compartments (*arrowheads*) and at the cell surface (*arrows*). After treatment with SST-14, cell surface proteins were transported from the cell surface into a cellular compartment localized directly beneath the plasma membrane (*yellow*, *arrowheads*). After 30 min, biotinylated proteins were transported from the cell surface into vesicles scattered throughout the cytoplasm (*arrowheads*). C, Higher magnification of nonstimulated cells. D, Higher magnification of a cell 30 min after stimulation with SST-14. *Arrowheads* indicate internalized sst1 present immediately beneath the cell membrane. *Bar*, 10 μm.

Intracellular sst1 is located in endocytic and recycling vesicles

To further evaluate the subcellular localization of intracellular sst1-HSV, RIN-sst1-HSV cells were transiently transfected with EGFP-coupled Rab5a and Rab11a. The function of Rab proteins in the conventional endocytosis and recycling pathway are well understood. Rab proteins are small GTPases that are involved in the formation of organized membrane domains. Rab proteins cycle between an active, GTP-bound and an inactive, GDP-bound state. Rab5a functions as a regulatory factor in the early endocytic pathway (32) and participates in endocytosis and intracellular trafficking of receptors as well as the fusion of early endosomes (33–35). Expression of inactive, GTP-binding-deficient Rab5aS34N partially inhibit translocation of transferrin from the plasma membrane to endosomes and cause accumulation of the neurokinin receptor 1 in vesicles located beneath the plasma membrane.

Rab11a is used as a marker protein for recycling vesicles and mediates the vesicular transport from late endosomes and early sorting endosomes to the plasma membrane. Rab11a also mediates the induced transport of vesicles from the Golgi apparatus to the plasma membrane (24, 36, 37). Expression of wild-type Rab11a and GTP-binding-deficient Rab11aS25N markedly impeded resensitization of neurokinin receptor 1. Therefore, we sought to investigate sst1-HSV trafficking by overexpressing cells with Rab5a-EGFP and Rab11a-EGFP.

Rab5a-mediated trafficking of sst1-HSV. In untreated cells, Rab5a-EGFP was present in perinuclear vesicular structures (Fig. 4). Although our earlier experiment showed that sst1-HSV was present at the cell surface and in intracellular compartments, under these conditions we found that sst1-HSV substantially colocalized with Rab5a-EGFP. Overexpression of Rab5a-EGFP markedly changed the distribution and size of sst1-HSV vesicles. Compared with untransfected cells, sst1-HSV appeared in larger vesicles concentrated at the perinuclear region.

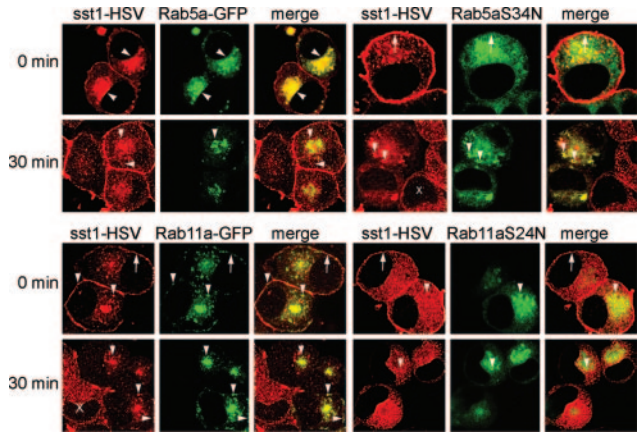

FIG. 4. Localization of sst1-HSV with marker proteins of endocytotic and recycling pathway. sst1-HSV (*red*) cells expressing Rab-EGFP proteins (*green*) were stimulated for 0 or 30 min with SST-14 (10 nM). Localization of sst1-HSV and Rab5a-EGFP, 0 min, sst1-HSV was present at the cell surface and strongly colocalized with Rab5a in a perinuclear compartment (*arrowheads*). After SST-14 stimulation, intracellular resident sst1 was also found separated from Rab5a. Localization of sst1-HSV and Rab5aS34N-EGFP, 0 min, sst1-HSV was present at the cell surface and colocalized with Rab5aS34N. Stimulation with SST-14 induced internalization of sst1-HSV. The receptor remained colocalized with Rab5aS34N. Localization of sst1-HSV and Rab11a-EGFP, 0 min, sst1-HSV was located at the cell surface (*arrows*) and extensively colocalized with Rab11a in intracellular compartments (*arrowheads*). After SST-14 stimulation, sst1-HSV was localized in Rab11a-positive vesicles located directly beneath the plasma membrane and scattered throughout the cell (*arrowheads*). sst1-HSV was not longer present at the cell surface. Localization of sst1-HSV and Rab11a S24N-EGFP, 0 min, sst1-HSV is located at the cell membrane and partially colocalized with Rab11aS24N. Stimulation induced internalization of sst1-HSV. *Bar*, 10 μm.

Stimulation with SST-14 did not markedly change the localization of Rab5a-EGFP but did change the localization of sst1-HSV, which was present in vesicles scattered throughout the cytoplasm (Fig. 4). These vesicles did not colocalize with the early endosome marker, Rab5a. sst1-HSV was also found at the cell surface under these conditions.

The pattern of sst1 trafficking was distinctly altered by coexpression of Rab5aS34N-EGFP (Fig. 4). In untreated cells, sst1 was localized at the cell surface and in vesicular structures. Rab5aS34N-EGFP was diffusely distributed in cytoplasmic vesicles, in which it partially colocalized with sst1. After stimulation with SST-14, internalized and intracellular sst1-HSV was found trapped and strongly associated within Rab5aS34N-EGFP-positive compartments. Expression of GTP-binding-deficient Rab5aS34N markedly changed sst1 trafficking. In cells expressing Rab5aS34N, surface localization of sst1 was lower than in cells that did not express Rab5aS34N (Fig. 4).

The results we obtained with confocal microscopy showed that intracellular sst1-HSV was partially colocalized with Rab5a, indicating its distribution in endocytic vesicles. Expression of GTP-binding-deficient Rab5aS34N strongly inhibited the intracellular vesicular transport of sst1-HSV. Expression of Rab5aS34N did not block receptor endocytosis. The distribution of sst1-HSV and Rab5aS34N within compartments localized beneath the cell membrane clearly demonstrates that Rab5a participates in sst1 trafficking. Because internalized and intracellular sst1 was found trapped and strongly associated within Rab5aS34N-EGFP-positive compartments, we suggest that stimulation with the agonist has recruited intracellular sst1-HSV to the plasma membrane and that continuous stimulation induced internalization of recruited sst1 and trapping of internalized sst1.

Rab11a mediated trafficking of sst1. In untreated cells, Rab11a was present in perinuclear vesicles and in vesicles located directly beneath the plasma membrane (Fig. 4). sst1-HSV was present at the cell surface and partially colocalized with Rab11a in perinuclear and superficial compartments (Fig. 4). Here it substantially colocalized with Rab11a-EGFP. Overexpression of Rab11a-EGFP markedly changed the distribution and size of sst1-HSV vesicles. Compared with RIN-sst1-HSV cells, sst1-HSV was localized within larger vesicles located in a perinuclear compartment. After 30 min of stimulation, sst1-HSV was markedly redistributed from the plasma membrane to Rab11a-positive compartments (Fig. 4). Expression of Rab11a-EGFP clearly altered trafficking of sst1-HSV. Cell surface location of sst1-HSV was markedly diminished by overexpression of Rab11a. Sst1-HSV remained colocalized within Rab11a-positive vesicles.

Expression of Rab11aS25N did not significantly affect endocytosis and trafficking of sst1. In nonstimulated cells, Rab11aS24N was diffusely located in the cytosol and large vesicular-like structures surrounding the perinuclear compartment of the cell (Fig. 4). sst1 was located at the cell membrane and in small vesicles scattered throughout the cytoplasm. sst1 immunoreactivity is slightly enhanced within Rab11aS34N-positive vesicles. Stimulation with SST-14 did not significantly change the localization of Rab11aS24N-EGFP. sst1 immunoreactivity was diminished at the cell membrane, indicating endocytosis of the receptor.

Confocal microscopy of Rab11a and Rab11aS24N in RIN-sst1-HSV cells showed that intracellular sst1 was also located in the recycling pathway of those cells. The results indicate that Rab11a participates in sst1 trafficking in both the recycling of receptors from superficial vesicles and the induced translocation of intracellular receptors to the cell surface. Our finding that intracellular sst1-HSV colocalized with Rab5a and Rab11a indicates that sst1-HSV is distributed in vesicles involved in endocytosis and recycling. Furthermore, the distribution of sst1-HSV within recycling vesicles suggests that intracellular sst1-HSV can be rapidly mobilized during stimulation to restore sst1 located on the cell surface.

Discussion

This study provides evidence that agonist-induced endocytosis of sst1-HSV is a dynamic process of endocytosis, recycling, and reendocytosis of intact and biologically active SST-14. We found that during chronic stimulation, SST-14 continuously accumulated in the cells and that accumulation was mediated by cell surface binding sites in steady state. This accumulation was accomplished by the mobilization of intracellularly present receptors and by endocytosed receptors that recycled to the plasma membrane. Colocalization of intracellular sst1-HSV with marker proteins of the endocytic and postendocytic pathways supported the assumption that stimulation with the agonist induced recruitment of intra-

cellular sst1. Interestingly, endocytosed SST-14-FITC was located only within superficial compartments. The rapid recycling of intact and biological active SST-14 after the medium was refreshed, and the uptake of surface-located sst1-HSV in a superficial compartment indicate that SST-14 is not routed into a lysosomal degradation pathway.

In contrast with our results in rat sst1, human sst1 did not or only slowly mediated an uptake of somatostatin, and stimulation of sst1 induced up-regulation of sst1 located on the cell surface (17–20). In our study, incubation of stimulated cells at 37 C allowed rapid release of internalized ligand. The rapid sst1-mediated uptake and reendocytosis of SST-14, along with the observation that SST-14 rapidly dissociated from the receptor in a neutral environment, indicates that sst1-induced endocytosis cannot be assessed by pulse-chase stimulation or after incubating the cells with acidic buffer at 37 C. Therefore, we suggest that differences in the methods used to quantify internalization of human and rat sst1 are responsible for the reported species-specific trafficking of sst1. This suggestion is supported by the results of confocal microscopy, which demonstrate bright immunoreactivity of both human and rat sst1 within the cytoplasm and that human and rat sst1 accumulate FITC-SST-14 into a representative superficial compartment (15, 18, 19, 22).

The ability to internalize and recycle intact somatostatin has also been reported for sst2a (38). We propose that the mechanisms leading to endocytosis and intracellular trafficking of sst2a are different from those reported for sst1. Endocytosis of sst2a but not sst1 is strongly associated with β-arrestins (22). Similarly, we could not demonstrate the involvement of β-arrestin in sst1-HSV internalization (data not shown). A comparison of both receptor subtypes with regard to receptor-mediated uptake of radiolabeled SST and transport of FITC-SST-14 showed that 75% of the specifically bound radioactivity was cell associated in sst2a-expressing cells and 20% was cell associated in sst1-expressing cells (determined after incubating the cells for 10 min at 37 C in acidic buffer) (18). Marked differences were found in the pattern of receptor-mediated transport of FITC-SST-14. Thus, sst2a transports FITC-SST-14 probably via early and late endosomes into the perinuclear compartment, whereas sst1 mediates the transport of the FITC-labeled peptide agonist into vesicular structures localized immediately beneath the plasma membrane (18).

Recent data from sst1 gene-deficient mice indicate a significant increase of somatostatin levels in the retina and up-regulation of sst2 expression. On the basis of these data, Dal Monte *et al.* (13) suggested that sst1 regulates the release of somatostatin and that the biological function of sst1 is that of an autoreceptor. The suggestion that sst1 controls the release of SST is supported by immunofluorescence data demonstrating that sst1 is preferentially localized presynaptically in axons containing SST and that sst1 is coexpressed with SST-14 in amacrine cells (11, 12, 39, 40).

A common feature of GPCR adjustment is down-regulation of the receptor during chronic stimulation. This was demonstrated for sst3, the muscarinic acetylcholine receptor, and the β-adrenergic receptor (41–43). Down-regulation may serve to protect cells against inappropriately intense or repeated stimulation.

Chronic stimulation of sst1 with high concentrations of SST-14 has not been shown to induce down-regulation of sst1 (15, 19). We suggest that chronic stimulation may not induce down-regulation of autoreceptors because down-regulation would result in a massive release of the ligand. Furthermore, in our study sst1 did not terminate the signal by routing the ligand to lysosomal degradation. The peptide was rapidly recycled as intact and biologically active SST-14. Considered as an autoregulative function of sst1 these transport mechanism may assure that the internalized peptide is returned into the extracellular fluid. By that means, the peptide agonist can maintain its sustained action on the target cell.

Acknowledgments

We thank Dr. M. Zerial for the Rab constructs and Dr. V. Gerke for critically reading the manuscript.

Received November 29, 2006. Accepted December 7, 2006.

Address all correspondence and requests for reprints to: Dr. D. Roosterman, Department of Dermatology and Ludwig Boltzmann Institute for Cell and Immunobiology of the Skin, Von-Esmarch-Str. 58, D-48148 Münster, Germany. E-mail: roosterman@gmx.net.

This work was supported by Sonderforschungsbereich (SFB) 492, SFB 293 A14 (to M.S.) and IZKF Münster II/103/04 (to M.S. and D.R.), and DK39957 (to N.W.B.).

Disclosure Statement: The authors have nothing to disclose.

References

1. **Olias G, Viollet C, Kusserow H, Epelbaum J, Meyerhof W** 2004 Regulation and function of somatostatin receptors. J Neurochem 89:1057–1091
2. **Patel YC** 1999 Somatostatin and its receptor family. Front Neuroendocrinol 20:157–198
3. **Schonbrunn A** 1999 Somatostatin receptors present knowledge and future directions. Ann Oncol 10(Suppl 2):S17–S21
4. **Roosterman D, Glassmeier G, Baumeister H, Scherubl H, Meyerhof W** 1998 A somatostatin receptor 1 selective ligand inhibits Ca2+ currents in rat insulinoma 1046–38 cells. FEBS Lett 425:137–140
5. **Nunn C, Cervia D, Langenegger D, Tenaillon L, Bouhelal R, Hoyer D** 2004 Comparison of functional profiles at human recombinant somatostatin sst2 receptor: simultaneous determination of intracellular Ca2+ and luciferase expression in CHO-K1 cells. Br J Pharmacol 142:150–160
6. **Cervia D, Fiorini S, Pavan B, Biondi C, Bagnoli P** 2002 Somatostatin (SRIF) modulates distinct signaling pathways in rat pituitary tumor cells: negative coupling of SRIF receptor subtypes 1 and 2 to arachidonic acid release. Naunyn Schmiedebergs Arch Pharmacol 365:200–209
7. **Douziech N, Calvo E, Coulombe Z, Muradia G, Bastien J, Aubin RA, Lajas A, Morisset J** 1999 Inhibitory and stimulatory effects of somatostatin on two human pancreatic cancer cell lines: a primary role for tyrosine phosphatase SHP-1. Endocrinology 140:765–777
8. **Buscail L, Delesque N, Esteve JP, Saint-Laurent N, Prats H, Clerc P, Robberecht P, Bell GI, Liebow C, Schally AV** 1994 Stimulation of tyrosine phosphatase and inhibition of cell proliferation by somatostatin analogues: mediation by human somatostatin receptor subtypes SSTR1 and SSTR2. Proc Natl Acad Sci USA 91:2315–2319
9. **Beaudet A, Greenspun D, Raelson J, Tannenbaum GS** 1995 Patterns of expression of SSTR1 and SSTR2 somatostatin receptor subtypes in the hypothalamus of the adult rat: relationship to neuroendocrine function. Neuroscience 65:551–561
10. **Viollet C, Lanneau C, Faivre-Bauman A, Zhang J, Djordjijevic D, Loudes C, Gardette R, Kordon C, Epelbaum J** 1997 Distinct patterns of expression and physiological effects of sst1 and sst2 receptor subtypes in mouse hypothalamic neurons and astrocytes in culture. J Neurochem 68:2273–2280
11. **Helboe L, Stidsen CE, Moller M** 1998 Immunohistochemical and cytochemical localization of the somatostatin receptor subtype sst1 in the somatostatinergic parvocellular neuronal system of the rat hypothalamus. J Neurosci 18:4938–4945
12. **Helboe L, Moller M** 1999 Immunohistochemical localization of somatostatin receptor subtypes sst1 and sst2 in the rat retina. Invest Ophthalmol Vis Sci 40:2376–2382
13. **Dal Monte M, Petrucci C, Vasilaki A, Cervia D, Grouselle D, Epelbaum J, Kreienkamp HJ, Richter D, Hoyer D, Bagnoli P** 2003 Genetic deletion of somatostatin receptor 1 alters somatostatinergic transmission in the mouse retina. Neuropharmacology 45:1080–1092

14. **Mastrodimou N, Thermos K** 2004 The somatostatin receptor (sst1) modulates the release of somatostatin in rat retina. Neurosci Lett 356:13–16
15. **Roosterman D, Roth A, Kreienkamp HJ, Richter D, Meyerhof W** 1997 Distinct agonist-mediated endocytosis of cloned rat somatostatin receptor subtypes expressed in insulinoma cells. J Neuroendocrinol 9:741–751
16. **Roth A, Kreienkamp HJ, Nehring RB, Roosterman D, Meyerhof W, Richter D** 1997 Endocytosis of the rat somatostatin receptors: subtype discrimination, ligand specificity, and delineation of carboxy-terminal positive and negative sequence motifs. DNA Cell Biol 16:111–119
17. **Hukovic N, Panetta R, Kumar U, Patel YC** 1996 Agonist-dependent regulation of cloned human somatostatin receptor types 1–5 (hSSTR1–5): subtype selective internalization or upregulation. Endocrinology 137:4046–4049
18. **Nouel D, Gaudriault G, Houle M, Reisine T, Vincent JP, Mazella J, Beaudet A** 1997 Differential internalization of somatostatin in COS-7 cells transfected with SST1 and SST2 receptor subtypes: a confocal microscopic study using novel fluorescent somatostatin derivatives. Endocrinology 138:296–306
19. **Hukovic N, Rocheville M, Kumar U, Sasi R, Khare S, Patel YC** 1999 Agonist-dependent up-regulation of human somatostatin receptor type 1 requires molecular signals in the cytoplasmic C-tail. J Biol Chem 274:24550–24558
20. **Liu Q, Schonbrunn A** 2001 Agonist-induced phosphorylation of somatostatin receptor subtype 1 (sst1). Relationship to desensitization and internalization. J Biol Chem 276:3709–3717
21. **Luttrell LM, Lefkowitz RJ** 2002 The role of β-arrestins in the termination and transduction of G-protein-coupled receptor signals. J Cell Sci 115:455–465
22. **Tulipano G, Stumm R, Pfeiffer M, Kreienkamp HJ, Hollt V, Schulz S** 2004 Differential β-arrestin trafficking and endosomal sorting of somatostatin receptor subtypes. J Biol Chem 279:21374–21382
23. **Schmidlin F, Dery O, DeFea KO, Slice L, Patierno S, Sternini C, Grady EF, Bunnett NW** 2001 Dynamin and Rab5a-dependent trafficking and signaling of the neurokinin 1 receptor. J Biol Chem 276:25427–25437
24. **Roosterman D, Schmidlin F, Bunnett NW** 2003 Rab5a and rab11a mediate agonist-induced trafficking of protease-activated receptor 2. Am J Physiol Cell Physiol 284:C1319–C1329
25. **Kurzchalia TV, Dupree P, Parton RG, Kellner R, Virta H, Lehnert M, Simons K** 1992 VIP21, a 21-kD membrane protein is an integral component of trans-Golgi-network-derived transport vesicles. J Cell Biol 118:1003–1014
26. **Presky DH, Schonbrunn A** 1986 Receptor-bound somatostatin and epidermal growth factor are processed differently in GH4C1 rat pituitary cells. J Cell Biol 102:878–888
27. **Lucius R, Mentlein R** 1991 Degradation of the neuropeptide somatostatin by cultivated neuronal and glial cells. J Biol Chem 266:18907–18913
28. **Mentlein R, Dahms P** 1994 Endopeptidases 24.16 and 24.15 are responsible for the degradation of somatostatin, neurotensin, and other neuropeptides by cultivated rat cortical astrocytes. J Neurochem 62:27–36
29. **Daukas G, Zigmond SH** 1985 Inhibition of receptor-mediated but not fluid-phase endocytosis in polymorphonuclear leukocytes. J Cell Biol 101:1673–1679
30. **Shen L, Turner JR** 2005 Actin depolymerization disrupts tight junctions via caveolae-mediated endocytosis. Mol Biol Cell 16:3919–3936
31. **Dinter A, Berger EG** 1998 Golgi-disturbing agents. Histochem Cell Biol 109: 571–590
32. **Bucci C, Parton RG, Mather IH, Stunnenberg H, Simons K, Hoflack B, Zerial M** 1992 The small GTPase rab5 functions as a regulatory factor in the early endocytic pathway. Cell 70:715–728
33. **Christoforidis S, McBride HM, Burgoyne RD, Zerial M** 1999 The Rab5 effector EEA1 is a core component of endosome docking. Nature 397:621–625
34. **Miaczynska M, Zerial M** 2002 Mosaic organization of the endocytic pathway. Exp Cell Res 272:8–14
35. **Zerial M, McBride H** 2001 Rab proteins as membrane organizers. Nat Rev Mol Cell Biol 2:107–117
36. **Ullrich O, Reinsch S, Urbe S, Zerial M, Parton RG** 1996 Rab11 regulates recycling through the pericentriolar recycling endosome. J Cell Biol 135:913–924
37. **Roosterman D, Cottrell G, Schmidlin F, Steinhoff M, Bunnett NW** 2004 Recycling and resensitization of the neurokinin 1 receptor: influence of agonist concentration and RAB GTPases. J Biol Chem 279:30670–30679
38. **Koenig JA, Kaur R, Dodgeon I, Edwardson JM, Humphrey PP** 1998 Fates of endocytosed somatostatin sst2 receptors and associated agonists. Biochem J 336(Pt 2):291–298
39. **Helboe L, Moller M** 2000 Localization of somatostatin receptors at the light and electron microscopial level by using antibodies raised against fusion proteins. Prog Histochem Cytochem 35:3–64
40. **Schulz S, Handel M, Schreff M, Schmidt H, Hollt V** 2000 Localization of five somatostatin receptors in the rat central nervous system using subtype-specific antibodies. J Physiol Paris 94:259–264
41. **Koenig JA, Edwardson JM** 1994 Kinetic analysis of the trafficking of muscarinic acetylcholine receptors between the plasma membrane and intracellular compartments. J Biol Chem 269:17174–17182
42. **Valiquette M, Bonin H, Hnatowich M, Caron MG, Lefkowitz RJ, Bouvier M** 1990 Involvement of tyrosine residues located in the carboxyl tail of the human β2-adrenergic receptor in agonist-induced down-regulation of the receptor. Proc Natl Acad Sci USA 87:5089–5093
43. **Suzuki T, Nguyen CT, Nantel F, Bonin H, Valiquette M, Frielle T, Bouvier M** 1992 Distinct regulation of β1- and β2-adrenergic receptors in Chinese hamster fibroblasts. Mol Pharmacol 41:542–548

***Endocrinology* is published monthly by The Endocrine Society (http://www.endo-society.org), the foremost professional society serving the endocrine community.**